2013 IEEE/RSJ International Conference on
Intelligent Robots and Systems (IROS)
November 3-7, 2013. Tokyo, Japan

Uncertainty-driven Survey Path Planning for Bathymetric Mapping

Enric Galceran, Sharad Nagappa, Marc Carreras, Pere Ridao and Albert Palomer

Abstract— **We present a novel survey path planning technique which minimizes the robot's position uncertainty along the planned path while taking into account area coverage performance. The proposed technique especially targets bathymetric mapping applications and respects application constraints such as the desire to survey in parallel tracks and to avoid turns in the target area to maximize sonar measurements quality. While accounting for uncertainty in the survey planning process can lead to more accurate data products, existing survey planning tools typically ignore it. Our method bridges this gap using the saliency on an *a priori* map to predict how the terrain will affect the robot's belief at every point on the target area. Based on this magnitude, we provide an algorithm that computes the order in which to trace parallel tracks to cover the target area minimizing the overall uncertainty along the path. A particle filter keeps track of the robot's position uncertainty during the planning process and, in order to find useful loop-closures for mapping, crossing tracks that visit salient locations are added when the uncertainty surpasses a user-provided threshold. We test our method on real-world datasets collected off the coasts of Spain, Greece and Australia. We evaluate the expected robot's position uncertainty along the planned paths and assess their associated mapping performance using a bathymetric mapping algorithm. Results show that our method offers benefits over a standard lawnmower-type path both in terms of position uncertainty and map quality.**

I. INTRODUCTION

The measurement of underwater depth of lake or ocean floors is known as bathymetric mapping. Bathymetric mapping supports safe navigation, helps protect and monitor marine areas of biological interest and is key to geology, archaeology and military applications, to name a few. Thanks to technology breakthroughs in the last two decades, autonomous underwater vehicles (AUVs) have become a standard tool supporting these applications [1], [2], [3], [4]. AUVs provide high resolution maps thanks to near-bottom surveys and require little human supervision compared to their ship- or remotely operated vehicle (ROV)-assisted counterparts, and hence at a lower cost. Incorporating uncertainty when planning a survey path for an AUV mapping mission can lead to more accurate maps. This is because most bathymetric mapping algorithms rely on the vehicle pose estimates during a mission to build the map. Therefore, the more accurate the vehicle pose estimates are the more accurate the resulting map will be.

This research was sponsored by the Spanish government (COMAROB Project, DPI2011-27977-C03-02) and the MORPH EU FP7-Project under the Grant agreement FP7-ICT-2011-7-288704.

The authors are with the Underwater Robotics Research Center (CIRS), University of Girona, Girona, Spain. {enricgalceran,snagappa,marcc,pere,apalomer}@eia.udg.edu

While the general problem of path planning under uncertainty has been addressed in several research works (see Related Work below), little attention has been given to incorporating uncertainty when planning paths for area coverage. Moreover, no uncertainty-aware path planning algorithms account for the application constraints of bathymetric mapping, such as the desire to survey in parallel tracks and to avoid turns on the target area to maximize sonar readings quality and to find useful loop-closures for the mapping algorithm. In fact, off-the-shelf survey design tools typically plan a lawnmower-type path on the target area completely ignoring uncertainty. Optionally, one or more crossing tracks are then appended seeking to provide loop-closures for the mapping process. However, these crossing tracks are placed arbitrarily, again ignoring uncertainty.

Aiming to bridge this gap, we present a survey path planning technique which takes into account the robot's motion and sensing uncertainty and seeks to minimize this uncertainty along the planned path. Bathymetry sonars provide noisy, highly corrupted range measurements under pronounced orientation changes. Therefore, our method operates on a parallel track basis to confine turns to the boundaries of the target area. We compute the saliency for every point of an *a priori* bathymetry of the target area* using the saliency map [5], a tool borrowed from the Computer Vision community. Based on the saliency, we provide an algorithm to decide the order in which to trace the parallel tracks to minimize uncertainty while also keeping extra path length into account. Once the order is determined, the algorithm uses a particle filter with the *a priori* bathymetry and simulated multibeam sonar measurements to estimate the robot's position uncertainty. Whenever the uncertainty after a parallel track exceeds a user-provided threshold, a crossing track through a salient area is inserted, seeking to reduce uncertainty and to find useful loop-closures for mapping. This contrasts with traditional survey path planning methods, which concatenate arbitrarily placed crossing tracks to a lawnmower-type path.

We test our algorithm on real-world datasets collected off the Formigues islands in Spain; the Santorini island in Greece; and Tasmania in Australia. We calculate the position uncertainty along the planned paths using terrain-aided particle filter localization and compare them to standard lawnmower-type paths. Additionally, we compare the mapping performance of a path planned using our method to a standard survey path on one of the datasets using a bathymetric mapping algorithm. Results show that our

*It is common in marine robotics applications to have prior knowledge of the target area in the form of low resolution bathymetry. The objective of a mapping mission is usually to obtain a more refined data product.

method offers benefits in terms of position uncertainty and map quality over a standard lawnmower-type path.

II. RELATED WORK

A considerable body of recent research has addressed the problem of motion planning under uncertainty. However, these works mostly address the "start-to-goal" path planning problem rather than area coverage and do not account for the aforementioned particulars of bathymetric mapping.

Many researchers propose extensions to the sampling-based Rapidly-exploring Random Trees (RRTs) and Probabilistic Roadmaps (PRM) path planning algorithms [6], [7] to handle uncertainty. The RRT extensions by Melchior and Simmons and Kewlani et al. explicitly handle uncertainty associated with terrain parameters (e.g., friction) [8], [9]. By taking this uncertainty into account these planners try to avoid rough terrain. However, sensing or state observation uncertainty is not considered in these works. Generalizations of the RRTs and PRM algorithms were proposed by Chakravorty and Kumar to obtain hybrid hierarchical motion planners that are robust to the motion uncertainty and to the uncertainty in the environment [10]. However, the generalizations proposed in this work assume perfect knowledge about the state of the robot.

Other path planners focus on the uncertainty in the map of the environment to generate paths with minimum probability of collision with obstacles [11], [12], [13], [14].

Active perception algorithms increase robot localization efficacy by specifically considering the expected uncertainty of the localization algorithm while planning the next control input the robot will receive [15], [16], [17]. Particularly related to the underwater domain are the next-best-view visual simultaneous localization and mapping (SLAM) approach by Kim and Eustice [18] and the active localization technique using multibeam sonar by Fairfield and Wettergreen [19]. However, these algorithms select a control action to minimize uncertainty at the next stage, but do not optimize over an entire path.

Another class of approaches use Markov decision processes (MDPs) with motion uncertainty to define a global control policy over the entire workspace, providing a connection between planning and control [20]. In order to also include sensing uncertainty, partially observable Markov decision processes (POMDPs) can be used [21], [22], [23]. Although POMDPs are theoretically satisfactory, these approaches require the discretization of the environment, and as a result they suffer from scalability problems.

Some planners seek to maximize the probability of success or rather to minimize an expected cost by taking into account the sensing uncertainty [24], [25], [26], [27], [28]. However, these approaches, either implicitly or explicitly, assume that maximum likelihood measurements are received from the sensor. As a result, the probability distributions of the robot's state are only approximated. In [29], by considering the controller used to execute the path, the true *a priori* probability distributions of the robot's state along its future path can be computed. By using these probability distributions, this method can select a path among several candidates such that maximizes the probability of arrival to the goal and at the same time minimizes the probability of collision.

In relation to the graph structure we use to represent parallel tracks, coverage path planning algorithms for environments that can be represented as a graph, such as a street or road network, were presented in [30]. However, uncertainty is not considered in this work.

III. UNCERTAINTY-DRIVEN SURVEY PATH PLANNING

As previously stated, in this work we deal with the application constraints of surveying the target area in parallel tracks and avoiding turns in the target area in order to maximize the quality of the sonar readings. We therefore operate on a parallel track basis by constructing a graph representing the parallel tracks required to cover the target area, which we call the coverage graph. Then, we plan a survey path in the two following steps:

1) Find the best possible order in which to cover the parallel track edges of the graph which minimizes the overall uncertainty along the path;
2) Insert crossing track edges in the path found in the first step if, after tracing a parallel track, the uncertainty surpasses a given threshold.

Finding the order in which to trace the parallel track edges raises two important concerns that need to be addressed. First, note that finding the optimal coverage path implies dealing with $n!$ candidate solutions, for a graph with n edges, which is an intractable problem [31]. Therefore, finding the optimal solution is computationally infeasible and some heuristic must be applied in order to find a good approximation in reasonable time. Second, commonly used heuristics do not apply to this problem due to the expansion and contraction of uncertainty (that is, the uncertainty through the path is non-monotonic). We address these concerns by determining the parallel track order based on the saliency of the terrain, which can be computed quickly. Then, we keep track of the robot's belief uncertainty along the determined path using a particle filter. When the estimated uncertainty surpasses a user-provided threshold, a crossing track that visits salient locations of the terrain is inserted, seeking to reduce the uncertainty.

Next, we first describe the construction of the coverage graph (Sec. III-A). Then, we discuss how the saliency map is used to compute the average saliency associated to each parallel track and to determine salient locations upon which to trace crossing tracks (Sec. III-B). The vehicle and measurement models and the particle filter algorithm used to keep track of the robot's position uncertainty are described in Sec. III-C and Sec. III-D, respectively. Finally, we describe our proposed survey path planning algorithm (Sec. III-E), which builds upon the coverage graph, the saliency map, the models and the particle filter.

A. Coverage Graph Construction

We construct a coverage graph consisting of equally spaced, parallel edges (tracks) with vertices lying on their endpoints. The vertices on each side of the parallel edges are then linked with the other vertices on the same side by vertical edges, forming a connected graph. In this work we consider tracks at a certain constant altitude from the seafloor, which together with the sonar swath aperture determine the inter-track spacing. Fig. 2 shows the coverage graphs on the datasets we later use to test our algorithm.

B. Saliency Calculation

When using the terrain's elevation profile for localization and/or mapping, we observe that profile measurements are less uncertain where the terrain is more salient. Based on this observation, in this work we propose to use the saliency map [5] over the *a priori* bathymetry as an estimation of the effect of the terrain on the robot's belief uncertainty. The saliency map assigns a saliency score to every pixel in an image (the bathymetry in this case).

We use the saliency map in two respects. First, for each parallel track, we compute the average saliency score in the rectangle determined by the bathymetry sonar footprint and the parallel track itself. Second, we determine key salient points through which our algorithm will later trace crossing tracks. We select regions surpassing a user-provided saliency threshold δ on the saliency map and take the weighted centroid of each high-saliency region as a key point. Fig 1 shows the saliency map and its corresponding segmentation ($\delta = 0.5$) and key salient points for the Formigues islands dataset.

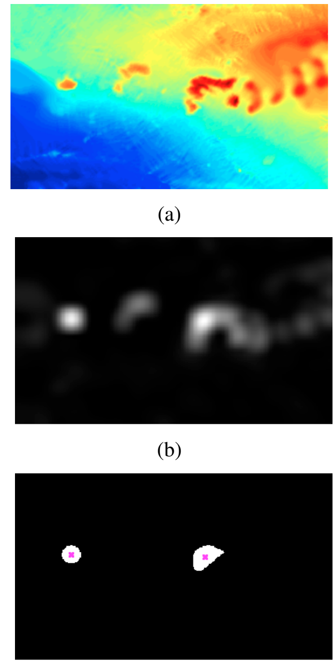

(a) (b) (c)

Fig. 1: Saliency computation for a bathymetric map (a): saliency map (b) and saliency map segmentation with $\delta = 0.5$ and the weighted centroids of each region marked as "x" (c).

C. Vehicle and Measurement Models

Given a bathymetric map, $\mathcal{B}$, and a path to be analyzed defined as a sequence of K 3-dimensional waypoints, $\Pi = [x_0, y_0, z_0]^\top, [x_1, y_1, z_1]^\top, ..., [x_K, y_K, z_K]^\top$, we define a vehicle model and a measurement model as follows.

1) Vehicle Model: The state vector s_t of the vehicle model is the 3 degrees of freedom (DOFs) vehicle position at path step k:

$$s_k = [x_k, y_k, z_k]^\top. \tag{1}$$

This state vector is updated according to a constant-velocity vehicle model

$$s_k = f(s_{k-1}, u_k) + \mathcal{N}(0, \sigma_f), \tag{2}$$

$$f(s_{k-1}, u_k) = s_{k-1} + u_k, \tag{3}$$

where u_k is the control vector at step k, in this case determined by the last and current path steps

$$u_k = \Pi_k - \Pi_{k-1} \tag{4}$$

and σ_f is additive Gaussian noise.

2) Measurement Model: We model a typical multibeam sonar providing an array of beams spread in a downward-facing swath perpendicular to the vehicle's direction of travel. At path step k, the vector of beam measurements is given by $\boldsymbol{r}_k = [r_{k,1}, \ldots, r_{k,N}]^\top$ and the measurement model for each beam i is given by

$$r_{k,i} = \mathcal{B}_i(x, y) - d_k + \mathcal{N}(0, \sigma_r), \forall 1 \leq i \leq N, \tag{5}$$

where $\mathcal{B}_i(x, y)$ is the map elevation at the point where the sonar beam i intersects the map surface, N is the number of beams, d_k is the vehicle's depth and σ_r is measurement noise which is assumed to be Gaussian. We simulate the sonar beams by shooting multiple rays against the map and computing their intersections.

D. Particle Filter

We use a particle filter based on the the SIR (sequential importance resampling) filter [32] to estimate the position and uncertainty of the robot along a given path Π. The distribution on the state s_k is approximated by the weighted set of particles $s_k^{(i)}, w_k^{(i)}, i \in [1, M]$ as

$$p(s_k|\boldsymbol{R}_k) = \sum_{i=1}^{M} w_k^{(i)} \delta_{s_k^{(i)}}(s_k), \tag{6}$$

where $\boldsymbol{R}_k = \boldsymbol{r}_{0:k}$. The particle weights are recursively updated according to the equations [32]

$$\hat{w}_k^{(i)} = w_{k-1}^{(i)} \frac{p(s_k^{(i)} | s_{k-1}^{(i)}) g(\boldsymbol{r}_k | s_k^{(i)})}{q(s_k^{(i)} | \boldsymbol{s}_{k-1}^{(i)}, \boldsymbol{R}_k)}, \tag{7}$$

$$w_k^{(i)} = \frac{\hat{w}_k^{(i)}}{\sum_{i=1}^{M} \hat{w}_k^{(i)}} \tag{8}$$

where the prior $p(s_k^{(i)} | s_{k-1}^{(i)})$ is given by Eq. (2), $q(\cdot|\cdot)$ represents the proposal distribution and $g(\cdot|\cdot)$ represents the likelihood function. Here, we use the prior distribution as the proposal distribution which results in simplification of the weight update. The particles are sampled according to

$$s_k^{(i)} \sim \mathcal{N}(f(s_{k-1}^{(i)}, u_k), \sigma_f^2 \mathbb{I}_3), \quad i \in [1, M]. \tag{9}$$

The likelihood function is given by

$$g(\boldsymbol{r}_k | s_k^{(i)}) = \mathcal{N}(\boldsymbol{r}_k; \hat{\boldsymbol{r}}_k^{(i)}, \sigma_r^2 \mathbb{I}_N) \tag{10}$$

where $\hat{\boldsymbol{r}}_k^{(i)}$ is the vector of expected elevations:

$$\hat{\boldsymbol{r}}_k^{(i)} = [\hat{r}_{k,1}^{(i)}, \ldots, \hat{r}_{k,N}^{(i)}], \tag{11}$$

$$\hat{r}_{k,i} = \mathcal{B}_i(x_k^{(i)}, y_k^{(i)}) - d_k. \tag{12}$$

Resampling with replacement is carried out at each time to limit the degeneracy of the particles.

In this work, we are interested only in the uncertainty of the robot's belief rather than in the position estimate. We estimate the uncertainty by evaluating the trace of the sample covariance of the distribution $p(s_k | \boldsymbol{R}_k)$ as

$$tr(\Sigma_k) = tr(\frac{1}{M-1} \sum_{i=1}^{M} (s_k^{(i)} - \bar{s}_k)(s_k^{(i)} - \bar{s}_k)^T). \tag{13}$$

E. Survey Path Planning Algorithm

Our survey path planning algorithm addresses the aforementioned intractability and application constraints with a saliency-based heuristic.

It first sorts the n parallel track edges in two groups of $\frac{n}{2}$ or $\frac{n}{2} - 1$ edges each: one with the highest saliency edges and one with lowest saliency edges (the edges being scored as described in Sec. III-B). Then it alternatively selects one edge from each group. The idea behind this heuristic is that the uncertainty growth incurred by a low saliency edge will be compensated by the high saliency of the next edge, avoiding high uncertainty peaks. To take also path distance into account, the closest edge on the next group is selected at every step.

To further bound the uncertainty, the algorithm estimates the robot's position uncertainty by tracing the parallel tracks in the order determined by the heuristic using the particle filter. If, after a track, the uncertainty surpasses a user-provided threshold α, a crossing track through the closest key salient point is inserted before continuing on the next parallel track.

It is worth noticing that our heuristic, inherently, does not guarantee an optimal path with respect to uncertainty. However, it tackles the intractability of the planning problem by producing a low uncertainty solution, as demonstrated by our experimental results (see Sec. IV below). On the other hand, small values of the uncertainty threshold α can lead to lengthened paths due to the addition of multiple crossing tracks seeking to reduce the uncertainty. However, our results show that a reasonably restrictive value of α does not lengthen the resulting path significantly. The choice of α strongly depends on the uncertainty tolerance of the target application. Evaluation of the effect of several values of α on the path produced by the algorithm can be used to determine a good fit for the application at hand.

The survey planning algorithm is detailed in Algorithm 1. The parallel track edges are classified in two groups according to their average saliency in line 2 (a low saliency group, E_L, and a high saliency group, E_H). The particle filter's particles, P, and weights, W, are initialized according to some initial distribution (line 4). `PopClosestNextEdge()` alternatively selects the closest edge from each group according to the h flag (line 8), and removes it from the group. In contrast, `GetClosestNextEdge()` accesses the appropriate edge, but does not remove it from the group (line 13).

Algorithm 1: Minimum Uncertainty Survey Path Planning

Input: List of parallel track edges in the coverage graph, E. *A priori* bathymetry, $\mathcal{B}$.
Parameters: Uncertainty threshold, α.
1 $\mathcal{S} \leftarrow$ `SaliencyMap`($\mathcal{B}$)
2 $(E_L, E_H) \leftarrow$ `ClassifyEdges`(E,$\mathcal{S}$)
3 $K \leftarrow$ `KeySalientPoints`($\mathcal{S}$)
4 $(P, W) \leftarrow$ `InitParticleFilter`()
5 $\hat{\Pi} \leftarrow \emptyset$
6 $h \leftarrow$ **true**
7 **while not** E_L*.empty()* **and** E_H*.empty()* **do**
8     $e \leftarrow$ `PopClosestNextEdge`(E_L,E_H,h)
9     $h \leftarrow$ **not** h
10     $\hat{\Pi}$.append(e)
11     $(P, W, \Sigma_k) \leftarrow$ `ParticleFilter`(e,P,W)
12   **if** $tr(\Sigma_k) > \alpha$ **then**
13         $n \leftarrow$ `GetClosestNextEdge`(E_L,E_H,h)
14         $c \leftarrow$ `BuildCrossingTrack`(e,n,K)
15         $\hat{\Pi}$.append(c)
16 **return** $\hat{\Pi}$

IV. RESULTS

We show the effectiveness of our proposed method in regions of interest of three different real-world bathymetric datasets collected at sea. For each dataset, we generate a survey path using our method and compare its performance to a standard lawnmower-type path. For the comparison, we simulate the path execution and keep track of the robot's belief using the particle filter algorithm presented above.

Additionally, on one of the datasets, we compare the effect on mapping performance of the paths planned using our method to a standard survey path planning method.

A. Datasets

The three bathymetric datasets upon which we evaluate our proposed planning method were collected: 1) near the Formigues islands off Girona, Spain, in the Mediterranian Sea; 2) in the Santorini caldera, Greece, in the Aegean Sea; and 3) off the island of Tasmania, Australia, in the Pacific Ocean. The Formigues and Santorini datasets were collected by our team in 2009 and 2012, respectively. The Tasmania dataset, recorded in 2009, was kindly provided by the School of Aerospace Mechanical and Mechatronic Engineering of the University of Sydney [33]. Fig. 2 shows the three datasets with their coverage graphs and their key salient points, obtained using a saliency threshold $\delta = 0.5$. The parallel tracks keep a constant 6 m altitude from the bottom and the inter-track spacing is determined by the footprint of a down-looking $120°$ swath aperture multibeam sonar. The Formigues islands dataset, shown in Fig. 2(a) was collected in a shallow coastal area; the Santorini dataset, shown in Fig. 2(b), was collected on an underwater volcanic site spreading from 290 m down to 360 m depth; the Tasmania dataset, shown in Fig. 2(c) was collected in a region including several hydrothermal vents.

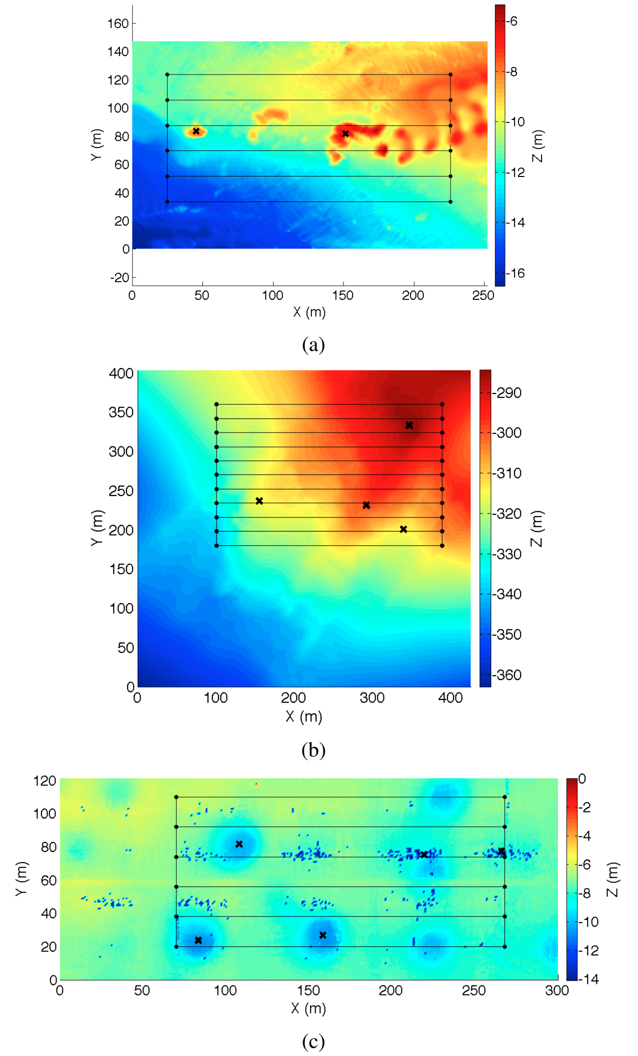

Fig. 2: Bathymetric datasets upon which we test out algorithm, with their corresponding coverage graph and key salient points (marked as "x"): (a) Formigues islands dataset, (b) Santorini dataset, (c) Tasmania dataset.

B. Position Uncertainty Results

We run our algorithm on each dataset, using the coverage graphs depicted in Fig. 2, with an uncertainty threshold $\alpha = 20$. We compare the paths planned using our method with a standard lawnmower-type path, the construction of which is well-documented in the literature [34], [35]. We append the same number of equally-spaced crossing tracks to the standard survey path as crossing tracks are inserted by our algorithm.

Fig. 3 shows the belief uncertainty, $tr(\Sigma_k)$, and its mean vs. path length for a standard lawnmower-type path and a path planned using our proposed method on each dataset. It can be observed that our method produces a path with a lower average uncertainty than the standard lawnmower-type path. We also notice that our method tends to avoid the high uncertainty peaks present in the standard lawnmower-type path. Regarding path length, our crossing track insertion procedure lengthens the path due to the requirement of visiting a (potentially distant) key salient point. However, the enhancement in navigation quality compensates the extra path length.

C. Mapping Results

We next compare the mapping performance associated to a path planned using the method proposed in this paper to the mapping performance of a standard survey path on the Formigues islands dataset.

We do so by executing the paths in simulation using UWSim [36], an open source tool for visualization and high-fidelity simulation of underwater robotic missions. UWSim allows us to use models of our GIRONA 500 AUV [37], a multi beam sonar and a navigation sensor suite to collect a complete bathymetric dataset in simulation. Moreover, UWSim is seamlessly integrated with GIRONA 500's control architecture [38], which means that the very same software that runs onboard the AUV in real missions is used in our simulations.

After executing the paths in simulation we apply a mapping algorithm to the multibeam sonar data collected along the paths. Once the maps are constructed we assess their quality and compare the results obtained using each type of path. We use the mapping algorithm by Zandara et al. [39] to build the bathymetric map and assess the map error. The map error is calculated as the standard deviation of the map points lying in every cell of a 3-dimensional grid. The maps obtained with our method and with the standard survey path

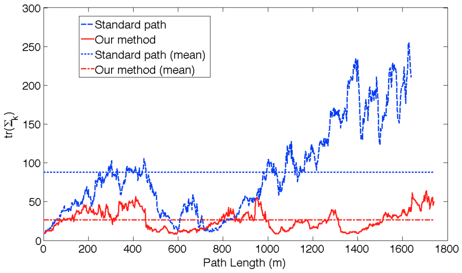

(a)

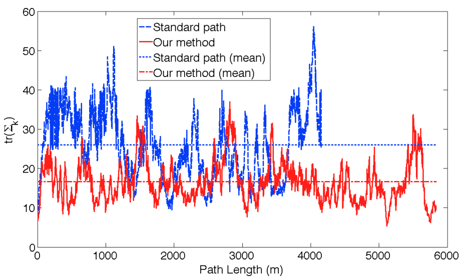

(b)

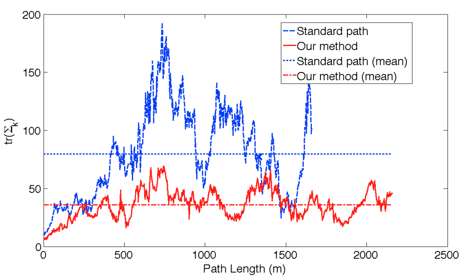

(c)

Fig. 3: Belief uncertainty, $tr(\Sigma_k)$, evolution and mean vs. path length for a standard lawnmower-type path and a path planned using our proposed method on each dataset: (a) Formigues islands dataset, (b) Santorini Caldera dataset, (c) Tasmania pockmarks dataset.

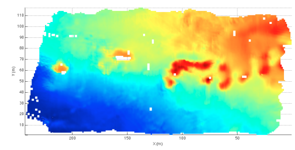

(a) Map (standard survey path)

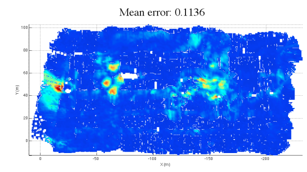

(b) Mapping error (standard survey path)

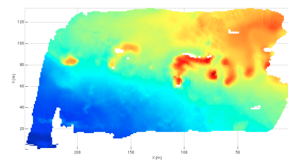

(c) Map (our method)

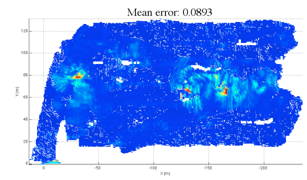

(d) Mapping error (our method)

Fig. 4: Mapping results for the Formigues islands dataset: map obtained with a standard lawnmower-type path (a) and its corresponding map error (b); map obtained with the path planned using our method (c) and its corresponding map error (d).

are shown in Fig. 4 together with their associated map errors. The path planned using our method produces a higher quality map, with an average map error of $0.0893\,\mathrm{m}$ in contrast to the average error of $0.1136\,\mathrm{m}$ produced by the standard survey path.

V. CONCLUSION AND FURTHER WORK

In this paper, we proposed a survey path planning method for area coverage aimed at minimizing uncertainty which takes into account the application constraints of bathymetric mapping. We compared the proposed method performance to standard lawnmower-type paths in terms of position uncertainty along the path on three different real-world datasets. Additionally, we compared the mapping performance associated to our method to a standard survey path using a bathymetric mapping algorithm. Results showed the benefit of incorporating uncertainty in the survey path planning phase both in terms of position uncertainty and mapping quality enhancement. Although this work focuses on bathymetric mapping, we believe that many underwater robotic applications can benefit from the techniques presented in this paper, especially those relying on the AUV trajectory estimate such as optical and sonar mosaicing. Likewise, data products obtained with different sensors, such as forward-looking and side-scan sonars, can benefit from the improved trajectory estimates enabled by our planning method.

Our method can easily be integrated into common survey planning tools for marine robotics, such as MB-System [40], which is freely available to the scientific community. The integration of the method presented in this paper can endow the users with a tool that capitalizes on the benefits of incorporating uncertainty in the survey planning. Therefore, immediate efforts will explore this possibility. Further work will consider incorporating *a priori* map errors into the robot's belief estimation, thereby accounting for the uncertainty in the environment's map. Exploring the theoretical uncertainty and optimality bounds of the proposed method is also a topic for future work. Finally, we would like to study the possibility of using multi-objective optimization techniques to balance the trade off between uncertainty and path length in our planning method.

REFERENCES

[1] J. Escartin, R. Garcia, O. Delaunoy, J. Ferrer, N. Gracias, A. Elibol, X. Cufi, L. Neumann, D. J. Fornari, S. E. Humphris, and J. Renard, "Globally aligned photomosaic of the lucky strike hydrothermal vent field (mid-atlantic ridge, 37 deg 18.5 min n): Release of georeferenced data, mosaic construction, and viewing software," *Geochemistry, Geophysics, Geosystems*, vol. 9, no. 12, pp. n/a–n/a, 2008. [Online]. Available: http://dx.doi.org/10.1029/2008GC002204

[2] B. Bingham, B. Foley, H. Singh, R. Camilli, K. Delaporta, R. Eustice, A. Mallios, D. Mindell, C. N. Roman, and D. Sakellariou, "Robotic tools for deep water archaeology: Surveying an ancient shipwreck with an autonomous underwater vehicle," *J. Field Robotics*, vol. 27, no. 6, pp. 702–717, 2010.

[3] D. R. Yoerger, D. S. Kelley, and J. R. Delaney, "Fine-scale three-dimensional mapping of a deep-sea hydrothermal vent site using the jason rov system," *The International Journal of Robotics Research*, vol. 19, no. 11, pp. 1000–1014, 2000. [Online]. Available: http://ijr.sagepub.com/content/19/11/1000.abstract

[4] D. P. Williams, "On optimal auv track-spacing for underwater mine detection," ICRA, pp. 4755–4762, 2010.

[5] L. Itti, C. Koch, and E. Niebur, "A model of saliency-based visual attention for rapid scene analysis," *Pattern Analysis and Machine Intelligence, IEEE Transactions on*, vol. 20, no. 11, pp. 1254–1259, 1998.

[6] S. M. LaValle and J. J. Kuffner, "Rapidly-exploring random trees: Progress and prospects," in *Proceedings Workshop on the Algorithmic Foundations of Robotics*, 2000.

[7] L. Kavraki, P. Svestka, J.-C. Latombe, and M. Overmars, "Probabilistic roadmaps for path planning in high-dimensional configuration spaces," *Robotics and Automation, IEEE Transactions on*, vol. 12, no. 4, pp. 566 –580, aug 1996.

[8] N. Melchior and R. Simmons, "Particle rrt for path planning with uncertainty," in *Robotics and Automation, 2007 IEEE International Conference on*, april 2007, pp. 1617 –1624.

[9] G. Kewlani, G. Ishigami, and K. Iagnemma, "Stochastic mobility-based path planning in uncertain environments," in *Intelligent Robots and Systems, 2009. IROS 2009. IEEE/RSJ International Conference on*, oct. 2009, pp. 1183 –1189.

[10] S. Chakravorty and S. Kumar, "Generalized sampling-based motion planners," *Systems, Man, and Cybernetics, Part B: Cybernetics, IEEE Transactions on*, vol. 41, no. 3, pp. 855 –866, june 2011.

[11] P. Missiuro and N. Roy, "Adapting probabilistic roadmaps to handle uncertain maps," in *Robotics and Automation, 2006. ICRA 2006. Proceedings 2006 IEEE International Conference on*, may 2006, pp. 1261 –1267.

[12] B. Burns and O. Brock, "Sampling-based motion planning using uncertain knowledge," University of Massachusetts at Amherst, Tech. Rep., 2006.

[13] L. Guibas, D. Hsu, H. Kurniawati, and E. Rehman, "Bounded uncertainty roadmaps for path planning," in *Proceedings of the Workshop on Algorithmic Foundations of Robotics*, 2008.

[14] A. Nakhaei and F. Lamiraux, "A framework for planning motions in stochastic maps," in *Control, Automation, Robotics and Vision, 2008. ICARCV 2008. 10th International Conference on*, dec. 2008, pp. 1959 –1964.

[15] W. Burgard, D. Fox, and S. Thrun, "Active mobile robot localization by entropy minimization," in *Advanced Mobile Robots, 1997. Proceedings., Second EUROMICRO workshop on*, 1997, pp. 155–162.

[16] N. Roy, W. Burgard, D. Fox, and S. Thrun, "Coastal navigation-mobile robot navigation with uncertainty in dynamic environments," in *Robotics and Automation, 1999. Proceedings. 1999 IEEE International Conference on*, vol. 1, 1999, pp. 35–40 vol.1.

[17] R. Valencia, J. Miro, G. Dissanayake, and J. Andrade-Cetto, "Active pose slam," in *Intelligent Robots and Systems (IROS), 2012 IEEE/RSJ International Conference on*, oct. 2012, pp. 1885 –1891.

[18] A. Kim, "Active visual slam with exploration for autonomous underwater navigation," Ph.D. dissertation, The University of Michigan, 2012.

[19] N. Fairfield and D. Wettergreen, "Active localization on the ocean floor with multibeam sonar," in *OCEANS 2008*, 2008, pp. 1–10.

[20] R. Alterovitz, T. Simeon, and K. Goldberg, "The stochastic motion roadmap: A sampling framework for planning with markov motion uncertainty," in *Robotics: Science and Systems III (Proc. RSS 2007)*, 2007.

[21] H. Kurniawati, D. Hsu, and W. Lee, "Sarsop: Efficient point-based pomdp planning by approximating optimally reachable belief spaces," in *Proceedings of the Robotics: Science and Systems*, 2008.

[22] S. Candido and S. Hutchinson, "Minimum uncertainty robot path planning using a pomdp approach," in *Intelligent Robots and Systems (IROS), 2010 IEEE/RSJ International Conference on*, oct. 2010, pp. 1408 –1413.

[23] J. van den Berg, S. Patil, and R. Alterovitz, "Motion planning under uncertainty using iterative local optimization in belief space," *The International Journal of Robotics Research*, vol. 31, no. 11, pp. 1263–1278, 2012. [Online]. Available: http://ijr.sagepub.com/content/31/11/1263.abstract

[24] R. Pepy and A. Lambert, "Safe path planning in an uncertain-configuration space using rrt," in *Intelligent Robots and Systems, 2006 IEEE/RSJ International Conference on*, oct. 2006, pp. 5376 –5381.

[25] J. Gonzalez and A. Stentz, "Using linear landmarks for path planning with uncertainty in outdoor environments," in *Intelligent Robots and Systems, 2009. IROS 2009. IEEE/RSJ International Conference on*, oct. 2009, pp. 1203 –1210.

[26] S. Prentice and N. Roy, "The belief roadmap: Efficient planning in belief space by factoring the covariance," *The International Journal of Robotics Research*, vol. 28, no. 11-12, pp. 1448–1465, November/December 2009. [Online]. Available: http://ijr.sagepub.com/content/28/11-12/1448.abstract

[27] R. Platt, R. Tedrake, L. Kaelbling, and T. Lozano-perez, "Belief space planning assuming maximum likelihood observations," in *Proceedings of the Robotics: Science and Systems*, 2010.

[28] H. Carrillo, Y. Latif, J. Neira, and J. Castellanos, "Fast minimum uncertainty search on a graph map representation," in *Intelligent Robots and Systems (IROS), 2012 IEEE/RSJ International Conference on*, 2012, pp. 2504–2511.

[29] J. van den Berg, P. Abbeel, and K. Goldberg, "Lqg-mp: Optimized path planning for robots with motion uncertainty and imperfect state information," *The International Journal of Robotics Research*, vol. 30, no. 7, pp. 895–913, 2011. [Online]. Available: http://ijr.sagepub.com/content/30/7/895.abstract

[30] L. Xu, "Graph planning for environmental coverage," Ph.D. dissertation, Carnegie Mellon University, 2011.

[31] G. Ausiello, P. Crescenzi, G. Gambosi, V. Kann, A. Marchetti-Spaccamela, and M. Protasi, *Complexity and Approximation. Combinatorial optimization problems and their approximability properties*. Springer Verlag, 1999.

[32] B. Ristic, S. Arulampalam, and N. Gordon, *Beyond the Kalman Filter*. Artech House, 2004.

[33] S. Barkby, S. Williams, O. Pizarro, and M. Jakuba, "Bathymetric particle filter slam using trajectory maps," *The International Journal of Robotics Research*, 2012. [Online]. Available: http://ijr.sagepub.com/content/early/2012/09/11/0278364912459666.abstract

[34] V. J. Lumelsky, S. Mukhopadhyay, and K. Sun, "Dynamic path planning in sensor-based terrain acquisition," *IEEE Transactions on Robotics and Automation*, vol. 6, no. 4, pp. 462–472, 1990.

[35] E. U. Acar, H. Choset, A. A. Rizzi, P. N. Atkar, and D. Hull, "Morse decompositions for coverage tasks," *International Journal of Robotics Research*, vol. 21, no. 4, pp. 331–344, 2002.

[36] M. Prats, J. Perez, J. Fernandez, and P. Sanz, "An open source tool for simulation and supervision of underwater intervention missions," in *Intelligent Robots and Systems (IROS), 2012 IEEE/RSJ International Conference on*, 2012, pp. 2577–2582.

[37] D. Ribas, N. Palomeras, P. Ridao, M. Carreras, and A. Mallios, "Girona 500 auv, from survey to intervention," *IEEE/ASME Transactions on Mechatronics*, vol. 17, no. 1, pp. 46–53, 2012.

[38] N. Palomeras, A. El-Fakdi, M. Carreras, and P. Ridao, "COLA2: A control architecture for AUVs," *Journal of Oceanic Engineering*, 2012.

[39] S. Zandara, P. Ridao, D. Ribas, A. Mallios, and A. Palomer, "Probabilistic surface matching for bathymetry based slam," in *Proceedings of the IEEE International Conference on Robotics and Automation*, Karlsruhe, Germany, May 2013.

[40] "Mb-system: Software for the processing and display of swath sonar data," http://www.mbari.org/data/mbsystem/, 2013, [Online; accessed 08-March-2013].